PHYSICAL REVIEW D **78,** 074508 (2008)

# First study of the three-gluon static potential in lattice QCD

M. Cardoso and P. Bicudo

*CFTP, Departamento de Física, Instituto Superior Técnico, Av. Rovisco Pais, 1049-001 Lisboa, Portugal*

(Received 10 July 2008; revised manuscript received 16 September 2008; published 15 October 2008)

We estimate the potential energy for a system of three static gluons in lattice QCD. This is relevant for the different models of three-body glueballs that have been proposed in the literature, either for gluons with a constituent mass, or for massless ones. A Wilson loop adequate to the static hybrid three-body system is developed. We study different spacial geometries, to compare the starfish model with the triangle model, for the three-gluon potential. We also study two different color structures, symmetric and antisymmetric, and compare the respective static potentials. A first simulation is performed in a $24^3 \times 48$ periodic Lattice, with $\beta = 6.2$ and $a \sim 0.072$ fm.

DOI: 10.1103/PhysRevD.78.074508 PACS numbers: 11.15.Ha, 12.38.Gc

## I. INTRODUCTION

We explore, in lattice QCD, the static potential of the three-body glueball system composed of three gluons, using Wilson loops. The interest in three-body gluon-gluon-gluon systems is increasing in anticipation of the future experiments BESIII at IHEP in Beijin, GLUEX at JLab, and PANDA at GSI in Darmstadt, dedicated to studying the mass range of charmonium, with a focus in its plausible excitations and in glueball production.

Even before the glueballs are discovered, the study of two-gluon and three-gluon glueballs are, respectively, relevant to the pomeron [1,2] and to the odderon [3]. Thus several models of three-gluon models have already started to be developed [3–12].

The relevance of computing the static potentials in lattice QCD for 3-gluon models is partly motivated by the plausible existence of a constituent mass for the gluon. Several evidences of a gluon effective mass of 600–1000 MeV, much larger than $\Lambda_{\rm QCD}$, exist from the lattice QCD gluon propagator in Landau gauge, [13,14], from Schwinger-Dyson and Bogoliubov-Valatin solutions for the gluon propagator in Landau gauge [15], from the analogy of confinement in QCD to superconductivity [16], from the lattice QCD breaking of the adjoint string [17], from the lattice QCD gluonic excitations of the fundamental string [18] from constituent gluon models [4,19,20] compatible with the lattice QCD glueball spectra [21–24], and with the Pomeron trajectory for high energy scattering [1,2]. Furthermore, even for modeling massless gluons, the knowledge of a static potential would at least provide one of the components of the dynamical potential. For instance, the static quark-antiquark potential, denominated funnel or Cornell potential, is frequently applied to light quarks, only with small corrections of the respective parameters [20,25]. This has been recently validated in lattice QCD, where the potential for a baryon made of two static quarks and a light one has been computed, [26,27] and indeed the part of the potential depending on the position of the light quark maintains the shape of the static potential, with corrected parameters.

The Wilson loop method was devised to extract, from pure-gauge QCD, the static potential for constituent quarks and to provide detailed information on the confinement in QCD. In what concerns gluon interactions, the first lattice studies were performed by Michael [17,28] and Bali extended them to other SU(3) representations [29]. Recently Okiharu and colleagues [30,31] studied for the first time another class of exotic hadrons, extending the Wilson loop of three-quark baryons to tetraquarks and to pentaquarks. Very recently, Bicudo, Cardoso, and Oliveira continued the lattice QCD mapping of the static potentials for exotic hadrons, with the study of the hybrid quark-antiquark-gluon static potential [32,33].

In this paper we study the three-gluon potentials in lattice QCD. We address two novel and important questions. Noticing that with three gluons two different color singlets can be constructed, symmetric or antisymmetric, we study whether the respective interactions are identical or different. This will be further detailed in Sec. II. Moreover, noticing that a gluon may couple to one adjoint string, or to a pair of fundamental strings, we study whether the potential is amenable to a triangle-shaped triplet of fundamental strings or to a starfish-shaped triplet of adjoint strings, as depicted in Fig. 1.

Notice that Kuzmenko, Shevchenko, and Simonov [11], using the vacuum correlator method, already studied the three-gluon system analytically. This study favors the tri-

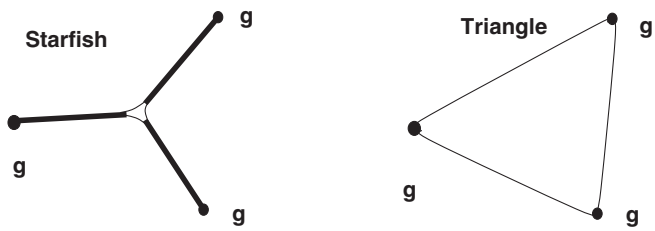


FIG. 1. The starfishlike and trianglelike possible geometries for the strings in the static three-gluon system.

 

angle (or ring) geometry over the starfish (or star) geometry. A prediction inspired in the bag model and in Casimir scaling (see for example [34]) suggests a starfish geometry but with a string tension that is $3/2\sigma$, instead of the $9/4\sigma$ of the adjoint string; however, it seems disfavored by lattice studies [29,32].

While the tree-gluon strings are only now being explored, the discussion on the shape of the baryonic strings has been addressed with detail in lattice QCD [35–45], including the study of the three-quark system at finite temperature [46].

In particular, our study of the hybrid system already indicated [32,33] that it would be interesting to study three-body glueballs, relevant for the odderon problem [3]. Notice that in lattice QCD, using the adjoint representation of SU(3), Bali [29] found that the adjoint string is compatible with the Casimir scaling, where the Casimir invariant $\lambda_i \cdot \lambda_j$ produces for the $gg$ interaction a factor $9/4$ times larger than the $q\bar{q}$ interaction. With three gluons, a triangle formed by three fundamental strings might cost less energy than three adjoint strings with a starfishlike geometry, depicted in Fig. 1. The three-gluon potential may be similar to a sum of three mesoniclike quark-antiquark interactions, plus a repulsion acting only when there is superposition of the fundamental strings. This question is also related to the superconductor (type-I vs type-II) model for confinement, where flux tubes repel each other in type-II superconductors, while in type-I superconductors they attract each other and tend to fuse in excited vortices [47]. A first evidence of QCD string repulsion was indeed found in our very recent study of the hybrid potential [32,33]. The understanding of the three-gluon potential in $3+1$-dimensional lattice QCD will further clarify our understanding of confinement.

In Sec. II we derive a class of Wilson loops adequate to study the static hybrid potential. This paper is mainly analytical, and in Sec. III we discuss theoretically the important questions of the best Wilson loops to distinguish the triangle from the starfish string ground states, and of the differences of the symmetric to antisymmetric potentials. In Sec. IV we present the first results of our numerical Monte Carlo simulations, and conclude.

## II. THREE-GLUON WILSON LOOP

We first construct a wave function with three gluons. This wave function will be the starting point of the Wilson loop. Because of confinement, a hadron, a system composed of quarks, antiquarks, or gluons, must be a color singlet.

Each gluon is a state of the adjoint, or octet **8**, representation of SU(3). With the tensor product of two gluons, different representations of SU(3) can be constructed,

$$\mathbf{8} \otimes \mathbf{8} = \mathbf{1} \oplus \mathbf{8} \oplus \mathbf{8} \oplus \mathbf{10} \oplus \mathbf{10} \oplus \mathbf{27} \tag{1}$$

including a singlet **1** and two octets **8**. When we couple three gluons, we get not just one color singlet, but two color singlets (plus many other representations), resulting from coupling this third octet to each of the two octets in the right-hand side of Eq. (1),

$$\mathbf{8} \otimes \mathbf{8} \otimes \mathbf{8} = \mathbf{1} \oplus \mathbf{1} \oplus \mathbf{8} \oplus \cdots \tag{2}$$

These two octets must have opposed symmetries, with one being symmetric for the permutation of two gluons, while the other is antisymmetric for gluon permutation. The symmetric one leads to charge conjugation $C = -$ three-gluon glueballs and the antisymmetric one leads to $C = +$ glueballs. To arrive at the wave function for the two color singlets, it is sufficient to study the product of two Gell-Mann matrices, since it already produces the relevant color singlet and color octets resulting from Eq. (1),

$$\lambda^a \lambda^b = \tfrac{2}{3}\delta^{ab} + i f_{abc}\lambda^c + d_{abc}\lambda^c, \tag{3}$$

and thus the product of three Gell-Mann matrices already produces the two possible color singlets, that we single out in the trace of the product of the three Gell-Mann matrices,

$$\mathrm{tr}\{\lambda^a \lambda^b \lambda^c\} = 2 i f_{abc} + 2 d_{abc}, \tag{4}$$

and thus the two possible color singlet wave functions of three gluons are

$$|\Psi^A\rangle = f_{abc}|abc\rangle, \qquad |\Psi^S\rangle = d_{abc}|abc\rangle, \tag{5}$$

where the first combination is antisymmetric and the second is symmetric with respect to the exchange of two gluons.

We build the three-gluon Wilson loop operator inspired in the three-quark case of the baryon. In the baryon we have a color singlet wave function given by

$$|\Psi^{\mathrm{Baryon}}\rangle = \epsilon_{ijk}|ijk\rangle, \tag{6}$$

and the corresponding Wilson loop is

$$W_{3q} = \epsilon_{ijk}\epsilon_{i'j'k'} X^{ii'} Y^{jj'} Z^{kk'}, \tag{7}$$

where $X$, $Y$, and $Z$ are the elementary paths of the three quarks, each composed of the product of successive elementary links $U$ starting and ending in wave functions of the form (6).

In the three-gluon-glueball case we proceed similarly, developing adjoint paths $\tilde{X}$, $\tilde{Y}$, and $\tilde{Z}$ starting either from the symmetric, or antisymmetric, color singlet wave functions (5), as illustrated in Fig. 2. Each adjoint path is composed of the product of successive adjoint links, corresponding to gluons, composed of matrices of the SU(3) adjoint or octet representation, given in terms of the fundamental representation ones by using the formula

$$\tilde{U}_\mu(x)^{ab} = \tfrac{1}{2}\mathrm{Tr}\{\lambda^a U_\mu(x) \lambda^b [U_\mu(x)]^\dagger\}. \tag{8}$$

Notice that these adjoint links are unitary matrices, as expected by a representation of SU(3),

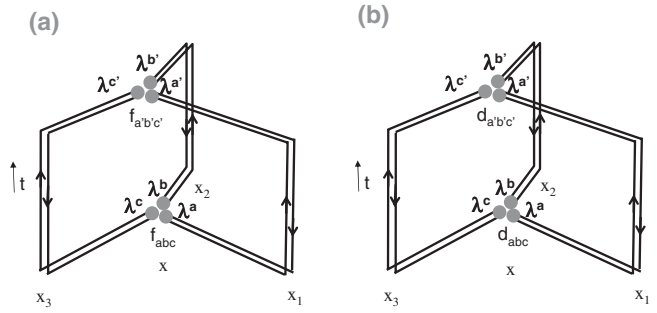


FIG. 2. Wilson loop for the $ggg$ potential, (a) for the symmetric color wave function and (b) for the antisymmetric color wave function.

$$\sum_b \tilde{U}^{ab}\tilde{U}^{\dagger bc} = \sum_b \frac{1}{4}\,\mathrm{Tr}[U^\dagger\lambda^a U\lambda^b]\mathrm{Tr}[\lambda^b U^\dagger\lambda^c U]$$
$$= \frac{1}{2}\,\mathrm{Tr}[U^\dagger\lambda^a U U^\dagger\lambda^c U] - \frac{1}{6}\,\mathrm{Tr}[U^\dagger\lambda^a U]Tr[U^\dagger\lambda^c U]$$
$$= \delta^{ac}, \tag{9}$$

where we used the Fierz relation,

$$\sum_a \lambda^a_{ij}\lambda^a_{kl} = 2\left(\delta_{il}\delta_{jk} - \frac{1}{3}\,\delta_{ij}\delta_{kl}\right) \tag{10}$$

illustrated in Fig. 3, to contract the $\lambda^b$ matrices.

We now explicitly derive the operator for the three-gluon Wilson loop. In the limit of arbitrarily large gluon masses, a nonrelativistic potential $V$ can be derived from the large time behavior of Euclidean time propagators. Typically, one has a meson operator $\mathcal{O}$ and computes the Green function,

$$\langle 0|\mathcal{O}(t)\mathcal{O}(0)|0\rangle \to \exp\{-Vt\} \tag{11}$$

for large $t$. Different types of operators allow the definition of different potentials. We can construct the three-gluon Wilson loop starting from the gluonic operator,

$$\mathcal{O}^A_{3g}(\mathbf{x}) = f_{abc}[g^a(\mathbf{x})][g^b(\mathbf{x})][g^c(\mathbf{x})], \tag{12}$$

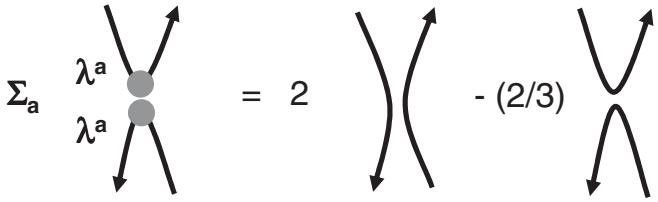


FIG. 3. Graphical version of the Fierz relation, showing that when two disconnect paths touch each other at the same point where a pair of Gell-Mann matrices is summed in their indices, this is equivalent to connecting the paths in two different ways, both gauge invariant.

where $g^a(\mathbf{x})$ is an operator that annihilates a gluon of color index $a$ at the position $\mathbf{x}$. The second operator $\mathcal{O}^S$ is constructed replacing $f_{abc}$ by $d_{abc}$.

In Eq. (12) the three octets are situated in the same point $\mathbf{x}$. Using the lattice links to comply with gauge invariance, the second operator in Eq. (12) can be made nonlocal to separate the three octet operators,

$$\mathcal{O}^A_{3g}(\mathbf{x},\mathbf{x}_1,\mathbf{x}_2,\mathbf{x}_3) = f_{abc}[\tilde{U}_{\mu_1}(\mathbf{x})\cdots\tilde{U}_{\mu_1}(\mathbf{x}+(r_1-1)\hat{\mu}_1)]^a{}_{a_1} \times g^{a_1}(\mathbf{x}+r_1\hat{\mu}_1)[U_{\mu_2}(\mathbf{x}) \cdots U_{\mu_2}(\mathbf{x} + (r_2-1)\hat{\mu}_2)]^b{}_{b_1} g^{b_1}(\mathbf{x}+r_2\hat{\mu}_2) \times [U_{\mu_3}(\mathbf{x})\cdots U_{\mu_3}(\mathbf{x}+(r_3-1)\hat{\mu}_3)]^c{}_{c_1} \times g^{c_1}(\mathbf{x}+r_3\hat{\mu}_3), \tag{13}$$

where we apply the lattice QCD prescription of linking the fields with links, to maintain the gauge invariance of our operator. We also assume the sum over repeated indices. The nonrelativistic potential requires the computation of the Green functions present in Eq. (11). Assuming that the Gluons are static, and that moreover any permutation of gluons is left for the future application of the present static potential in constituent gluon models, the contraction of the gluon field operators provides adjoint temporal links, giving rise to the gluon operator,

$$W^A_{3g} = f_{abc}f_{a'b'c'}[\tilde{U}_{\mu_1}(0,\mathbf{x})\cdots\tilde{U}_{\mu_1}(0,\mathbf{x}+(r_1-1)\hat{\mu}_1)\tilde{U}_4(0,\mathbf{x}+r_1\hat{\mu}_1)\cdots\tilde{U}_4(t-1,\mathbf{x}+r_1\hat{\mu}_1) \times \tilde{U}^\dagger_{\mu_1}(t,\mathbf{x}+(r_1-1)\hat{\mu}_1)\cdots\tilde{U}^\dagger_{\mu_1}(t,\mathbf{x})]^{aa'} \times [\tilde{U}_{\mu_2}(0,\mathbf{x})\cdots\tilde{U}_{\mu_2}(0,\mathbf{x}+(r_2-1)\hat{\mu}_2)\tilde{U}_4(0,\mathbf{x}+r_2\hat{\mu}_2)\cdots \times \tilde{U}_4(t-1,\mathbf{x}+r_2\hat{\mu}_2)\tilde{U}^\dagger_{\mu_2}(t,\mathbf{x}+(r_2-1)\hat{\mu}_2)\cdots\tilde{U}^\dagger_{\mu_2}(t,\mathbf{x})]^{bb'} \times [\tilde{U}_{\mu_3}(0,\mathbf{x})\cdots\tilde{U}_{\mu_3}(0,\mathbf{x}+(r_3-1)\hat{\mu}_3) \times \tilde{U}_4(0,\mathbf{x}+r_3\hat{\mu}_3)\cdots\tilde{U}_4(t-1,\mathbf{x}+r_3\hat{\mu}_3)\tilde{U}^\dagger_{\mu_3}(t,\mathbf{x}+(r_3-1)\hat{\mu}_3)\cdots\tilde{U}^\dagger_{\mu_3}(t,\mathbf{x})]^{cc'}. \tag{14}$$

We now translate the adjoint links into quark links. This is convenient, both to explicitly show that our Wilson loop is SU(3) gauge invariant, and to arrive at a more convenient expression for our computer simulations. So let us consider the product of two adjoint links, and apply again the Fierz relation to, say,

$$\sum_b \tilde{U}_1{}^{ab}\tilde{U}_2{}^{bc} = \sum_b \frac{1}{4}\,\mathrm{Tr}[U_1{}^\dagger\lambda^a U_1\lambda^b]\mathrm{Tr}[\lambda^b U_2\lambda^c U_2{}^\dagger] = 2\frac{1}{4}\,\mathrm{Tr}[U_1{}^\dagger\lambda^a U_1 U_2\lambda^c U_2{}^\dagger] - \frac{2}{3}\frac{1}{4}\,\mathrm{Tr}[U_1{}^\dagger\lambda^a U_1]\mathrm{Tr}[U_2\lambda^c U_2{}^\dagger]$$
$$= \widetilde{U_1 U_2}{}^{ac}. \tag{15}$$

Thus the product of two adjoint links is the adjoint of the product of two links. Iterating this result to the product of an arbitrary number of links, we get that all three paths present in Eq. (14) verify

$$[\tilde{U}_{\mu_1}(0,\mathbf{x})\cdots\tilde{U}^\dagger_{\mu_1}(t,\mathbf{x})]^{aa'} = \frac{1}{2}\,\mathrm{Tr}\{\lambda^a U_{\mu_1}(0,\mathbf{x})\cdots \times U^\dagger_{\mu_1}(t,\mathbf{x})\lambda^{a'}U_{\mu_1}(t,\mathbf{x})\cdots \times U^\dagger_{\mu_1}(0,\mathbf{x})\} = \frac{1}{2}\,\mathrm{Tr}\{\lambda^a X\lambda^{a'}X^\dagger\} = \tilde{X}, \quad (16)$$

where $X$ is the quark path utilized in the Wilson loop for static baryon potentials, corresponding to the gluon path $\tilde{X}$ In particular, the Wilson loop in Eq. (14) can be decomposed in quark paths $X$, $Y$, and $Z$, as in Fig. 2,

$$W^A_{3g} = f_{abc}f_{a'b'c'}\mathrm{Tr}\{\lambda^a X\lambda^{a'}X^\dagger\}\mathrm{Tr}\{\lambda^b Y\lambda^{b'}Y^\dagger\}\mathrm{Tr}\{\lambda^a Z\lambda^{c'}Z^\dagger\}, \quad (17)$$

$$W^S_{3g} = d_{abc}d_{a'b'c'}\mathrm{Tr}\{\lambda^a X\lambda^{a'}X^\dagger\}\mathrm{Tr}\{\lambda^b Y\lambda^{b'}Y^\dagger\}\mathrm{Tr}\{\lambda^a Z\lambda^{c'}Z^\dagger\}, \quad (18)$$

extending the three-quark Wilson loop of Eq. (7), replacing the quark fundamental SU(3) path $X$, by the gluon adjoint SU(3) path $\tilde{X}$. We also removed the overall $1/8$ factors since the potentials are independent of the norm of the Wilson loops.

We now proceed to completely translate the results of Eqs. (17) and (18) into fundamental quark paths. We express the Eqs. (17) and (18) in terms of correlations of the quark paths $X$, $Y$, and $Z$ only. Noticing

$$f_{abc} = \frac{1}{4i}\,\mathrm{Tr}\{(\lambda^a\lambda^b - \lambda^b\lambda^a)\lambda^c\}, \qquad d_{abc} = \frac{1}{4}\,\mathrm{Tr}\{(\lambda^a\lambda^b + \lambda^b\lambda^a)\lambda^c\}, \quad (19)$$

we replace in Eqs. (17) and (18) the structure functions $f_{abc}$ and $d_{abc}$ by traces of Gell-Mann matrices. Then we repeatedly apply the Fierz relation (10), illustrated in Fig. 3.

Subtracting and summing the results of the two different contractions of Fig. 4, we get the contribution of the respective symmetric and antisymmetric wave functions to the three-gluon Wilson loops,

$$\begin{aligned} f_{abc}\mathrm{Tr}[\lambda^a A]\,\mathrm{Tr}[\lambda^b B]\,\mathrm{Tr}[\lambda^c C] &= \frac{i}{2}\lambda^a_{ij}\lambda^b_{kl}(\lambda^b\lambda^a - \lambda^a\lambda^b)_{mn}A_{ji}B_{lk}C_{nm} \\ &= \frac{i}{2}(\lambda^a_{ij}\lambda^b_{kl}\lambda^b_{mp}\lambda^a_{pn} - \lambda^a_{ij}\lambda^b_{kl}\lambda^a_{mp}\lambda^b_{pn})A_{ji}B_{lk}C_{nm} \\ &= 2i(\mathrm{Tr}[CBA] - \mathrm{Tr}[ABC]), \end{aligned} \quad (20)$$

where we assumed a sum over repeated indices. Following

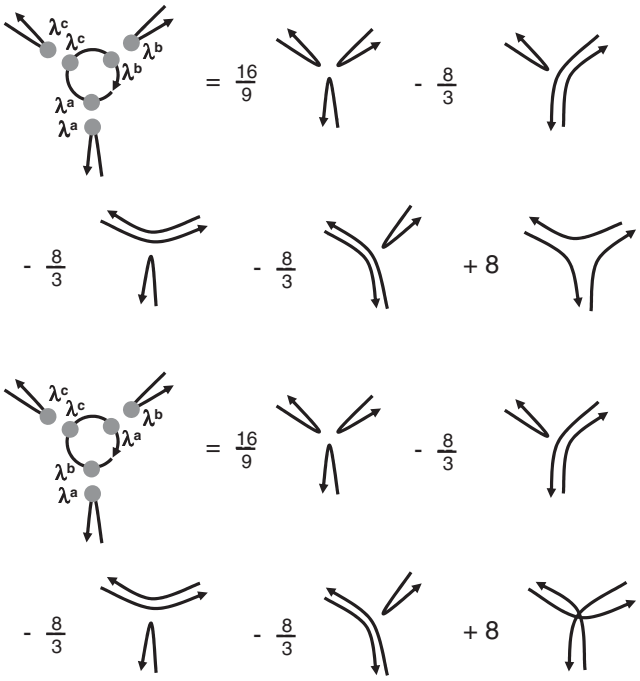


FIG. 4. Contractions of the three pairs of Gell-Mann matrices resulting from one of the three-gluon wave functions. This shows that the three-gluon Wilson loops, present in Eqs. (17) and (18), are gauge invariant, because they can be written as connected paths of lattice QCD links $U$.

a similar procedure we also get

$$f_{abc}\mathrm{Tr}[\lambda^a A\lambda^b B\lambda^c C] = 2i\mathrm{Tr}[A]\,\mathrm{Tr}[B]\,\mathrm{Tr}[C] - 2i\mathrm{Tr}[CBA]. \quad (21)$$

Using the results (20) and (21) we finally arrive at the expression for the Wilson loop for the antisymmetric color arrangement

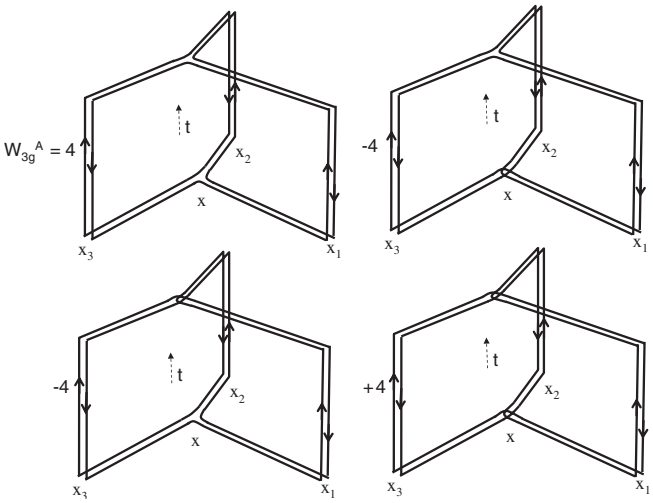


FIG. 5. The antisymmetric three-gluon Wilson loop $W^A_{3g}$ expressed with paths of quarklike fundamental $U$ links.

$$W^A_{3g} = +4\,\mathrm{Tr}[XY^\dagger]\,\mathrm{Tr}[YZ^\dagger]\,\mathrm{Tr}[ZX^\dagger] + 4\,\mathrm{Tr}[X^\dagger Y]\,\mathrm{Tr}[Y^\dagger Z]\,\mathrm{Tr}[Z^\dagger X] - 4\,\mathrm{Tr}[XZ^\dagger YX^\dagger ZY^\dagger] - 4\,\mathrm{Tr}[XY^\dagger ZX^\dagger YZ^\dagger], \quad (22)$$

depicted in Fig. 5. Using the same techniques for the operator for the symmetric color wave function,

$$\begin{aligned} d_{abc}\mathrm{Tr}[\lambda^a A]\,\mathrm{Tr}[\lambda^b B]\,\mathrm{Tr}[\lambda^c C] &= 2\,\mathrm{Tr}[ABC] + 2\,\mathrm{Tr}[CBA] - \tfrac{4}{3}\mathrm{Tr}[A]\,\mathrm{Tr}[BC] - \tfrac{4}{3}\mathrm{Tr}[B]\,\mathrm{Tr}[CA] - \tfrac{4}{3}\mathrm{Tr}[C]\,\mathrm{Tr}[AB] \\ &\quad + \tfrac{8}{9}\mathrm{Tr}[A]\,\mathrm{Tr}[B]\,\mathrm{Tr}[C], \\ d_{abc}\mathrm{Tr}[\lambda^a A\lambda^b B]\,\mathrm{Tr}[\lambda^c C] &= 2\,\mathrm{Tr}[AC]\,\mathrm{Tr}[B] + 2\,\mathrm{Tr}[BC]\,\mathrm{Tr}[A] + \tfrac{8}{9}\mathrm{Tr}[AB]\,\mathrm{Tr}[C] - \tfrac{4}{3}\mathrm{Tr}[ABC] - \tfrac{4}{3}\mathrm{Tr}[CBA] \\ &\quad - \tfrac{4}{3}\mathrm{Tr}[A]\,\mathrm{Tr}[B]\,\mathrm{Tr}[C], \\ d_{abc}\mathrm{Tr}[\lambda^a A\lambda^b B\lambda^c C] &= 2\,\mathrm{Tr}[CBA] + \tfrac{8}{9}\mathrm{Tr}[ABC] - \tfrac{4}{3}\mathrm{Tr}[A]\,\mathrm{Tr}[BC] - \tfrac{4}{3}\mathrm{Tr}[B]\,\mathrm{Tr}[CA] - \tfrac{4}{3}\mathrm{Tr}[C]\,\mathrm{Tr}[AB] \\ &\quad + 2\,\mathrm{Tr}[A]\,\mathrm{Tr}[B]\,\mathrm{Tr}[C], \end{aligned} \quad (23)$$

and finally we get,

$$W^S_{3g} = 4\,\mathrm{Tr}[XY^\dagger ZX^\dagger YZ^\dagger] + 4\,\mathrm{Tr}[X^\dagger ZY^\dagger XZ^\dagger Y] - \tfrac{16}{3}\mathrm{Tr}[XY^\dagger]\,\mathrm{Tr}[X^\dagger Y] - \tfrac{16}{3}\mathrm{Tr}[YZ^\dagger]\,\mathrm{Tr}[Y^\dagger Z] - \tfrac{16}{3}\mathrm{Tr}[ZX^\dagger]\,\mathrm{Tr}[Z^\dagger X] + 4\,\mathrm{Tr}[X^\dagger Y]\,\mathrm{Tr}[Y^\dagger Z]\,\mathrm{Tr}[Z^\dagger X] + 4\,\mathrm{Tr}[Y^\dagger X]\,\mathrm{Tr}[Z^\dagger Y]\,\mathrm{Tr}[X^\dagger Z] + \tfrac{32}{3}. \quad (24)$$

The results in terms of quarklike Wilson loops, composed of fundamental links only, are illustrated in Figs. 5 and 6.

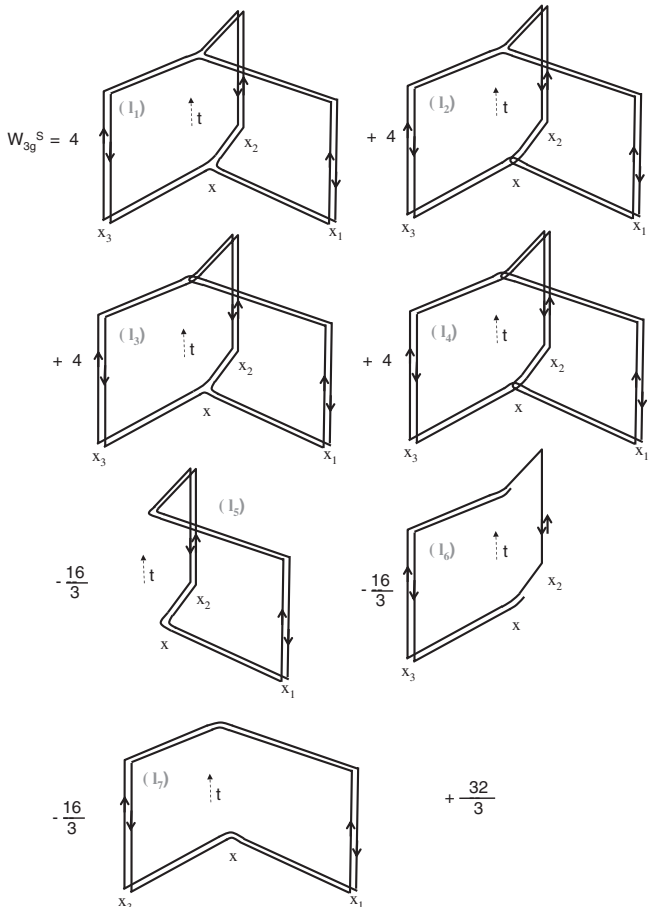


FIG. 6. The symmetric three-gluon Wilson loop $W^S_{3g}$ expressed with paths of quarklike fundamental $U$ links. Each individual loop is labeled by a $l_i$.

## III. ANALYTICAL DISCUSSION

The class of Wilson loops $W^A_{3g}$ and $W^S_{3g}$ formally derived in Sec. II still contain degrees of freedom, that we may use to increase the signal-to-noise ratio. In particular, the paths linking the fixed positions $\mathbf{x}_1$, $\mathbf{x}_2$, and $\mathbf{x}_3$ of the three gluons remain to be determined.

Notice that smearing is a standard technique to increase the signal-to-noise ratio of the Wilson loop. The smearing [48–53] of the spatial links is a technique consisting of repeatedly mixing a link to neighbor staplelike paths. The resulting mixing is unitarized back to a SU(3) matrix. The smearing is expected to maximize the signal- (of the ground state) to-noise ratio when the smearing is comparable to the actual width of the QCD confining flux tube.

Moreover, the Wilson loops $W^A_{3g}$ and $W^S_{3g}$ defined in Sec. II depend on the position of the point $\mathbf{x}$, initially defined in Eq. (12). Notice, however, that the actual static potential should not depend on this $\mathbf{x}$ point. Possibly, as long as we keep fixed the points $\mathbf{x}_1$, $\mathbf{x}_2$, and $\mathbf{x}_3$, the spatial paths connecting these points could also be arbitrarily changed, even if they do not meet in a common point $\mathbf{x}$; however this remains to be verified. Importantly, we expect that the spatial paths closer to the actual position of the strings confining the three gluons will maximize the signal-to-noise ratio.

In Fig. 7 we show two possible different spatial paths linking the points $\mathbf{x}_1$, $\mathbf{x}_2$, and $\mathbf{x}_3$. In this paper, for simplicity, we use only paths parallel to the lattice grid. In Fig. 7(a) we place the three gluons at the vertices of an equilateral triangle, constructed with the edges of a cube. Placing the vertex of the cube at, say (0,0,0), three points forming the triangle are $(r, 0, 0)$, $(0, r, 0)$, and $(0, 0, r)$. In Fig. 7(a), the $\mathbf{x}$ point is located at the simplest possible position for a numerical simulation, at the vertex (0,0,0) of the cube. In Fig. 7(b), the paths are quite simple; we place the three gluons at the vertices of an isosceles rect triangle,

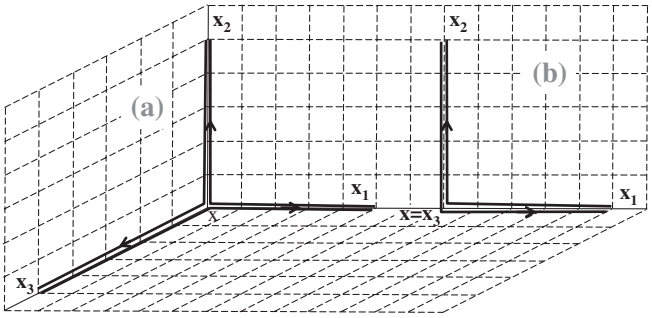


FIG. 7. Spatial paths, (a) for an equilateral triangle using the vertex of a cube, (b) for an isosceles rect triangle, using the vertex of a square.

and the $\mathbf{x}$ point coincides with the $\mathbf{x}_3$, thus the spatial geometry is planar. The paths in Figs. 7(a) and 7(b) are neither placed at the starfishlike string position, nor at the position of the trianglelike string position. More sophisticated choices of paths might lead to better signal-to-noise ratios, but the paths in Fig. 7 are the simplest for a first simulation.

On the other hand we may explore analytical similarities or differences between the Wilson loops $W^A_{3g}$ and $W^S_{3g}$. The Casimir scaling, dominating the perturbative QCD, and, at least, the short-distance potentials, can be algebraically computed,

$$\lambda_1 \cdot \lambda_2 = \frac{(\lambda_1 + \lambda_2 + \lambda_3)^2 - (\lambda_1{}^2 + \lambda_2{}^2 + \lambda_3{}^2)}{6} = -6, \tag{25}$$

and the result is the same both for the symmetric and the antisymmetric potentials. Thus the short-range part of the interactions should be identical.

Now we also check that in the limit where two gluons are superposed, we recover the normal two-gluon operator, where the result is proportional to (the proportionality factor is irrelevant here)

$$W_{gg} = W_{q\bar{q}} W_{q\bar{q}}{}^* - 1, \tag{26}$$

where, say, $W_{q\bar{q}} = \mathrm{Tr}\{XY^\dagger\}$ is a complete one-quark Wilson Loop. Thus when $x_3 = x_2$ or equivalently when $Z = Y$, we get, for the antisymmetric loop $W^A_{3g}$,

$$W^A_{3g} \to 24(WW^* - 1) \tag{27}$$

and are also identical in the symmetric loop $W^S_{3g}$,

$$W^S_{3g} \to \tfrac{40}{3}(WW^* - 1). \tag{28}$$

Importantly, since the result only differs in a physically irrelevant constant factor, this shows that whenever two of the arms of the starfish are superposed, the two potentials, for the symmetric and for the antisymmetric cases, are identical. Then, if any difference occurs, it only occurs when the arms are separated. Thus, we should position the gluons at the vertices of an open triangle, say an equilateral triangle, or an isosceles rect triangle, to study this possible difference.

## IV. NUMERICAL RESULTS

Since this is mainly an analytical paper, in Sec. IV we only numerically simulate the simplest paths to compute, with the spatial subpaths depicted in Fig. 7. We perform our simulations with 141 configurations generated by the Monte Carlo method in a $24^3 \times 48$ periodic lattice, with $\beta = 6.2$ and $a \sim 0.072$ fm.

First, we check that the sum of all the different quarklike Wilson loops vanish in the limit of large Euclidean time $t$. This actually happens, and we also numerically check that the Wilson loops, as described in Figs. 5 and 6, in the limit of large $t$ tend to

$$l_1 = l_2 = l_3 = l_4 \to \tfrac{1}{3}, \qquad l_5 = l_6 = l_7 \to 1. \tag{29}$$

Then, we study the possible difference between the antisymmetric and symmetric static potentials, defined in Figs. 5 and 6 and in Eqs. (22) and (24).

The results of our simulations for the difference between the antisymmetric and symmetric static potentials as a function of the perimeter $p = r_{12} + r_{23} + r_{31}$ are show in Fig. 8 and suggest a difference between the two potentials with the potential for the symmetric color arrangement being slightly larger than the one for the antisymmetric arrangement. To quantify this difference, we fit the difference between the two potentials to a constant plus linear function

$$V_{\mathrm{sym}} - V_{\mathrm{asym}} = C_{\mathrm{diff}} + \sigma_{\mathrm{diff}} p, \tag{30}$$

and obtain $\sigma_{\mathrm{diff}} = (0.043 \pm 0.003)\sigma$ ($\sigma$ is the fundamental string tension), with $\chi^2/\mathrm{dof} = 1.00$. The fit is made to all

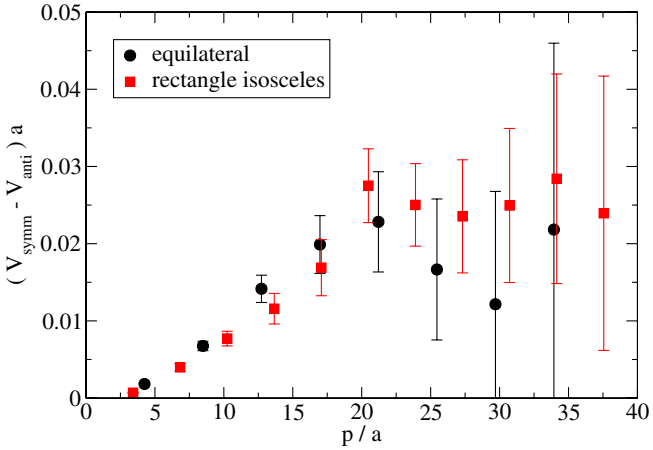


FIG. 8 (color online). We show the difference $V^S - V^A$ of the three-gluon potentials of the two operators $W^S_{3g}$ and $W^A_{3g}$ as a function of the perimeter $p$ of the respective triangle. For the spatial geometry of the loops, we utilize the equilateral triangle of Fig. 7(a).

points in both geometries with $p/a < 40$. It must be noted that, since the error bars of the last points are very large, as can be seen in Fig. 8, we cannot assert that the difference between the two potentials always rises linearly, it remains possible that the difference saturates at larger distances.

To verify that the static potentials do not depend on the arbitrary meeting point $\mathbf{x}$ of the spatial paths, we compute the static potentials for two different geometries, depicted in Fig. 7. In case (a), the point $\mathbf{x}$ is placed relatively far from the position of any of the three gluons. In case (b) the point $\mathbf{x}$ coincides with the position of one of the gluons. As anticipated in Sec. III, the potentials show little dependence on the point $\mathbf{x}$. This is illustrated in Fig. 9, where both geometries produce similar results.

We also study the two potentials separately, as defined in Figs. 5 and 6 and in Eqs. (22) and (24). The results for the potentials are shown in Fig. 9 as a function of the triangle perimeter

$$V_{\text{triangle}} = C + \sum_{i<j} -\frac{\alpha}{r_{ij}} + \sigma' p. \tag{31}$$

Notice that our study only aims at the confining part of the potential; for a precise study of the Coulomb potential we will need more statistics or different techniques [54]. Nevertheless, we obtain the results for the different color/geometry combinations in the fitting range $10 < p < 40$ shown in Table I.

This result clearly rules out the starfish model, since it would give us a string tension of $\sigma' = \frac{9}{4\sqrt{3}}\sigma \simeq 1.30\sigma$ for the equilateral triangle geometry and $\sigma' = \frac{9(1+\sqrt{3})}{8(1+\sqrt{2})}\sigma \simeq 1.27\sigma$ for the triangle rectangle isosceles geometry. It must be noted that the error of the string tension is of the same order or greater than $\sigma_{\text{diff}}$, calculated before. Nevertheless, since the difference $\sigma_{\text{diff}}$ is systematic, we are able to compute it.

TABLE I. Results of the fits for the various geometry and color arrangement combinations.

| Geometry/symmetry | $\sigma'/\sigma$ | $\alpha$ | $\chi^2$/dof |
|---|---|---|---|
| Equilateral/antissymetric | 1.04 ± 0.04 | 0.28 ± 0.03 | 1.07 |
| Equilateral/symmetric | 1.05 ± 0.06 | 0.29 ± 0.05 | 1.37 |
| Isosceles/antisymmetric | 1.07 ± 0.03 | 0.23 ± 0.02 | 0.92 |
| Isosceles/symmetric | 1.10 ± 0.13 | 0.23 ± 0.17 | 1.13 |

The results are also not compatible with the bag model, which would give us $\sigma' = \frac{\sqrt{3}}{2}\sigma \simeq 0.87\sigma$ and $\sigma' = \frac{3(1+\sqrt{3})}{4(1+\sqrt{2})}\sigma \simeq 0.85\sigma$ for the equilateral triangle and rect triangle geometries.

Finally, to check that the $24^3 \times 48$ lattice configurations are producing good results, we show the plot of $-\log W_{3g}$, which is used to calculate the potentials, in Fig. 10.

To conclude, we show that there are two, and only two, symmetric and antisymmetric, three-gluon static potentials. We derive the two respective Wilson loops and study them analytically. We perform numerical tests, verifying that our Wilson loop is correct. Notice that the three-gluon Wilson loops include products of up to three fundamental Wilson loops, technically difficult to compute. We thus leave the systematic numerical exploration of the three-gluon Wilson loops for future works. Nevertheless, our numerical simulations already indicate that the symmetric potential is slightly larger than the antisymmetric one, and that both are compatible with the trianglelike model for the three-gluon static potential.

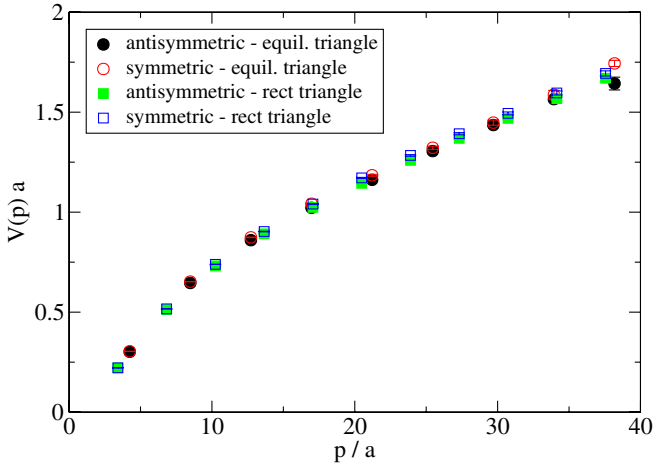


FIG. 9 (color online). We show the three-gluon potentials for the two operators ($W^A_{3g}$ and $W^S_{3g}$) as a function of the perimeter $p$ of the respective triangle. We utilize both the equilateral triangle and the isosceles rect triangle spatial paths of Figs. 7(a) and 7(b). The results are extracted from 141 SU(3) lattice QCD configurations $24^3 \times 48$, with the smearing of $100 \times 0.5$ in space and of $1 \times 1$ in time.

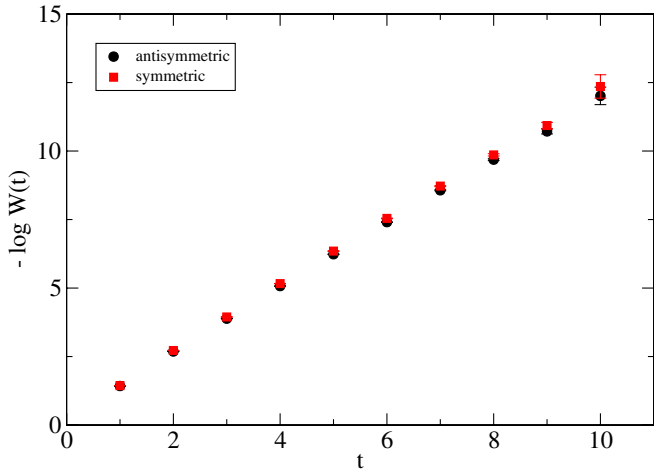


FIG. 10 (color online). Plots of $-\log W_{3g}$ for the two operators ($W^A_{3g}$ and $W^S_{3g}$), which we use to get the values of the potentials, for the equilateral triangle geometry with a perimeter $p = 15\sqrt{2}$ and for 141 lattice QCD configurations $24^3 \times 48$. In this simulation we use $100 \times 0.5$ smearing steps in space and $1 \times 1$ smearing step in time.

## ACKNOWLEDGMENTS

Part of the present work was funded by the FCT Grants No. PDCT/FP/63923/2005 and No. POCI/FP/81933/2007. We thank Orlando Oliveira for sharing with us his set of 141 configurations in a $24^3 \times 48$ SU(3)QCD lattice in part based on the MILC Collaboration's public lattice gauge theory code [55,56], and for scientific discussions.

[1] F. J. Llanes-Estrada, S. R. Cotanch, P. J. de A. Bicudo, J. E. F. Ribeiro, and A. P. Szczepaniak, Nucl. Phys. **A710**, 45 (2002).
[2] H. B. Meyer and M. J. Teper, Phys. Lett. B **605**, 344 (2005).
[3] F. J. Llanes-Estrada, P. Bicudo, and S. R. Cotanch, Phys. Rev. Lett. **96**, 081601 (2006).
[4] W. S. Hou and A. Soni, Phys. Rev. D **29**, 101 (1984).
[5] V. Mathieu, C. Semay, and B. Silvestre-Brac, Phys. Rev. D **74**, 054002 (2006).
[6] F. Buisseret and C. Semay, Phys. Rev. D **76**, 017501 (2007).
[7] V. Mathieu, C. Semay, and B. Silvestre-Brac, Phys. Rev. D **77**, 094009 (2008).
[8] A. B. Kaidalov and Yu. A. Simonov, Phys. Lett. B **477**, 163 (2000).
[9] A. B. Kaidalov and Yu. A. Simonov, Phys. Lett. B **636**, 101 (2006).
[10] Yu. A. Simonov, Phys. At. Nucl. **70**, 44 (2007).
[11] D. S. Kuzmenko, V. I. Shevchenko, and Yu. A. Simonov, arXiv:hep-ph/0310190.
[12] N. Boulanger, F. Buisseret, V. Mathieu, and C. Semay, arXiv:0806.3174.
[13] D. B. Leinweber, J. I. Skullerud, A. G. Williams, and C. Parrinello (UKQCD Collaboration), Phys. Rev. D **60**, 094507 (1999); **61**, 079901(E) (2000).
[14] P. J. Silva and O. Oliveira, Nucl. Phys. **B690**, 177 (2004).
[15] C. S. Fischer, R. Alkofer, and H. Reinhardt, Phys. Rev. D **65**, 094008 (2002).
[16] H. B. Nielsen and P. Olesen, Nucl. Phys. **B61**, 45 (1973).
[17] C. Michael, Nucl. Phys. **B259**, 58 (1985).
[18] L. A. Griffiths, C. Michael, and P. E. L. Rakow, Phys. Lett. **129B**, 351 (1983).
[19] A. Szczepaniak, E. S. Swanson, C. R. Ji, and S. R. Cotanch, Phys. Rev. Lett. **76**, 2011 (1996).
[20] E. Abreu and P. Bicudo, J. Phys. G **34**, 195 (2007).
[21] C. J. Morningstar and M. J. Peardon, Phys. Rev. D **60**, 034509 (1999).
[22] G. S. Bali, K. Schilling, A. Hulsebos, A. C. Irving, C. Michael, and P. W. Stephenson (UKQCD Collaboration), Phys. Lett. B **309**, 378 (1993).
[23] H. Chen, J. Sexton, A. Vaccarino, and D. Weingarten, Nucl. Phys. B, Proc. Suppl. **34**, 357 (1994).
[24] M. J. Teper, arXiv:hep-th/9812187.
[25] W. Lucha, F. F. Schoberl, and D. Gromes, Phys. Rep. **200**, 127 (1991).
[26] A. Yamamoto, H. Suganuma, and H. Iida, Phys. Lett. B **664**, 129 (2008).
[27] A. Yamamoto, H. Suganuma, and H. Iida, Phys. Rev. D **78**, 014513 (2008).
[28] N. A. Campbell, I. H. Jorysz, and C. Michael, Phys. Lett. **167B**, 91 (1986).
[29] G. S. Bali, Phys. Rev. D **62**, 114503 (2000).
[30] F. Okiharu, H. Suganuma, and T. T. Takahashi, Phys. Rev. D **72**, 014505 (2005).
[31] F. Okiharu, H. Suganuma, and T. T. Takahashi, Phys. Rev. Lett. **94**, 192001 (2005).
[32] P. Bicudo, M. Cardoso, and O. Oliveira, Phys. Rev. D **77**, 091504 (2008).
[33] M. Cardoso, P. Bicudo, and O. Oliveira, Proc. Sci. LAT2007 (2007) 293 [arXiv:0710.1762].
[34] G. Martens, C. Greiner, S. Leupold, and U. Mosel, Phys. Rev. D **70**, 116010 (2004).
[35] O. Jahn and P. de Forcrand, Nucl. Phys. B, Proc. Suppl. **129**, 700 (2004).
[36] Ph. de Forcrand and O. Jahn, Nucl. Phys. **A755**, 475 (2005).
[37] T. T. Takahashi and H. Suganuma, Phys. Rev. Lett. **90**, 182001 (2003).
[38] H. Suganuma, T. T. Takahashi, and H. Ichie, arXiv:hep-lat/0312031.
[39] H. Suganuma, H. Ichie, and T. T. Takahashi, arXiv:hep-lat/0407011.
[40] T. T. Takahashi and H. Suganuma, Phys. Rev. D **70**, 074506 (2004).
[41] A. Yamamoto and H. Suganuma, Phys. Rev. D **77**, 014036 (2008).
[42] H. Suganuma, A. Yamamoto, N. Sakumichi, T. T. Takahashi, H. Iida, and F. Okiharu, arXiv:0802.3500.
[43] A. Yamamoto, H. Suganuma, and H. Iida, arXiv:0805.4735.
[44] B. Silvestre-Brac, C. Semay, I. M. Narodetskii, and A. I. Veselov, Eur. Phys. J. C **32**, 385 (2003).
[45] F. Bissey, F. G. Cao, A. R. Kitson, A. I. Signal, D. B. Leinweber, B. G. Lasscock, and A. G. Williams, Phys. Rev. D **76**, 114512 (2007).
[46] K. Hubner, F. Karsch, O. Kaczmarek, and O. Vogt, Phys. Rev. D **77**, 074504 (2008).
[47] P. G. de Gennes, *Superconductivity of Metals and Alloys* (Addison-Wesley, Reading, MA, 1989).
[48] G. S. Bali, K. Schilling, and C. Schlichter, Phys. Rev. D **51**, 5165 (1995).
[49] G. Parisi, R. Petronzio, and F. Rapuano, Phys. Lett. **128B**, 418 (1983).
[50] M. Albanese *et al.* (APE Collaboration), Phys. Lett. B **192**, 163 (1987).
[51] F. Okiharu and R. M. Woloshyn, Eur. Phys. J. C **35**, 537 (2004).
[52] T. T. Takahashi, H. Suganuma, Y. Nemoto, and H. Matsufuru, Phys. Rev. D **65**, 114509 (2002).

[53] G. S. Bali, H. Neff, T. Duessel, T. Lippert, and K. Schilling (SESAM Collaboration), Phys. Rev. D **71**, 114513 (2005).
[54] M. Caselle, M. Hasenbusch, and M. Panero, J. High Energy Phys. 01 (2003) 057.
[55] This work was in part based on the MILC Collaboration's public Lattice gauge theory code. See http://physics.indiana.edu/~sg/milc.html.
[56] T. Blum, C. DeTar, S. Gottlieb, K. Rummukainen, U. M. Heller, J. E. Hetrick, D. Toussaint, R. L. Sugar, and M. Wingate, Phys. Rev. D **55**, R1133 (1997).